ELSEVIER

PII: S0032-3861(96)00950-0

Polymer Vol. 38 No. 15, pp. 3783–3793, 1997

0032-3861/97/$17.00 + 0.00

Kinetics of ultrasonic and transient elongational flow degradation: a comparative study

Tuan Q. Nguyen*, Qi Z. Liang and Henning-H. Kausch
Swiss Federal Institute of Technology, Department of Materials Science, Polymer Laboratory, MX-D, CH-1015 Lausanne, Switzerland
(Received 13 March 1996; revised 12 July 1996)

The kinetics of ultrasonic degradation has been investigated for dilute polystyrene solutions in decalin. The increase in the scission rate constant (K) with initial molecular chain length was systematically investigated over 2 decades of molecular weight by using narrow polymer fractions with $M = 50 \times 10^3$–8.5×10^6 Da. An empirical relation of the form $K \sim (M - M_{lim})^{1.9}$, with $M_{lim} = 30\,000$, was found for $50 \times 10^3 \leq M \leq 2.2 \times 10^6$. The rate constant becomes independent from M at higher molecular weight. This complex behaviour is rationalized by establishing a parallelism between transient elongational flow and ultrasonic degradation. © 1997 Elsevier Science Ltd.

(Keywords: ultrasound; transient elongational flow; degradation)

INTRODUCTION

Ultrasonic and simple shear degradation have long been the two classical fields of studies in polymer chemistry[1,2]. More recent interests are focused on chain scission in elongational flow where flexible long macromolecular chains were believed to become highly extended before fracture[3,4]. A survey of published literature on mechanochemistry[1,5] reveals several distinct features which, interestingly enough, are common for elongational flow and for ultrasonic degradation. A sharp propensity for midchain scission was observed in both systems. In addition, it was determined that the rate of degradation showed a negative polymer concentration dependence which is only weakly influenced by the solution viscosity but increases in proportion to the energy input, i.e. the hydrodynamic energy for transient elongational flow and the sonication power for ultrasonic irradiation. Based on a mechanical model of frictional loading, it is predicted that the molecular stress increases with the square of polymer chain length in a constant velocity gradient[6]. This relation seems to be verified in stagnation point elongational flow where the critical strain rate for bond rupture ($\dot{\varepsilon}_f$) scales with polymer molecular weight (M) as $\dot{\varepsilon}_f \propto M^{-2.3}$. This seemingly coherent picture of mechanochemical degradation has been challenged by the recent results obtained in fast *transient* flow created by forcing a polymer solution across a convergent contraction. In contrast to opposed jets flow, which has a stagnation point at its symmetry centre, abrupt contraction flow has open flow lines, and, therefore, the residence time is limited along any streamline. Although the short residence time in convergent channels does not allow appreciable chain uncoiling, chain rupture was found to be almost quantitative with a sharp propensity for midchain scission. In addition, a weaker molecular weight dependence $\dot{\varepsilon}_f \propto M^{-1}$ was found in *transient* elongational flow[7]. This result was explained by the short residence time inherent to this type of flow which does not allow large degree of chain uncoiling.

From the preceding discussion, it seems that a precise determination of the degradation scaling exponent is essential to a molecular understanding of the chain scission mechanism. The influence of molecular weight on the rate of ultrasonic degradation is not without ambiguities. Using carefully refractionated aqueous solutions of dextran, Ederer *et al.* established a direct proportionality between the rate of ultrasonic degradation (K) and the polymer molecular weight[8]. Most experimental data on ultrasonication of synthetic polymers such as polystyrene (PS) revealed, however, a different trend, i.e. $K \propto M^{-2.9-11}$.

The kinetics of ultrasonic and transient elongational flow degradation presents so many similarities that a fortuitous coincidence seems to be unlikely. In light of the progress in the field of elongational flow, it seems desirable to repeat some of the earlier ultrasonic degradation experiments for a proper comparison and rationalization of chain scission mechanisms which occur in both systems.

EXPERIMENTAL

Chemicals

The used PS samples are narrow molecular weight standards from Polymer Laboratories (Shropshire, UK) with M_p (MW at peak maximum) in the range of 50×10^3–8.5×10^6 Da. The dispersity index, $\bar{M}_w/\bar{M}_n$, is < 1.05 for molecular weights below 4×10^6 but increases to 1.20 for the highest molecular weight polymer. Chemicals are from Fluka AG (Switzerland). Decalin is a mixture of 58% *trans*- and 41% *cis*-decahydronaphthalene + 1%

* To whom correspondence should be addressed

tetrahydronaphthalene as determined by gas chromatography. The polymer solutions are stirred gently for 24 h, then filtered through a 12 μm porous glass before use. The experimental θ temperature for PS in that solvent is 14.8°C[12]. The following Mark–Houwink–Sakurada (MHS) equations have been obtained for PS at the experimental temperature of 295 K:

$$[\eta] = 2.34 \times 10^{-3} M^{0.53} \text{ m}^3 \text{ kg}^{-1} \quad (1)$$

with M in units of kilograms per mole.

Ultrasonic degradation

Degradation was carried out at an ultrasonic frequency of 20 kHz with a Branson Sonifier (model 250/200 W). The ultrasound intensity was set to 10% (i.e. 20 W) of the maximum power. A 50 ml glass vessel filled with 25 ml of polymer solution was immersed in a water bath thermostatted at 22 ± 0.5°C. Five aliquots of 0.2 ml were taken at regular intervals for gel permeation chromatography (g.p.c.) analysis. The slight decrease in the irradiation volume due to sample withdrawal was neglected in the subsequent calculations. Ultrasonic intensity depended on the position of the irradiation horn; it is, therefore, essential to keep the test vessel unperturbed for the entire duration of experiments. In the course of degradation, free radicals are formed. In solution, these highly reactive species disappear rapidly by secondary reactions with dissolved impurities, by recombination or by radical transfer to the solvent molecules. In order to avoid these complications, it is common to use an efficient radical scavenger which can be either dissolved oxygen or some purposely added chemical species. The presence of dissolved air could have, however, a deleterious effect on the precision of the results. During the first few seconds of ultrasonication, dissolved gas will diffuse into the cavitation bubbles cushioning their collapse and decreasing the degradation yield. Moreover, the concentration of oxygen may decrease with time due to outgassing and changes in the rate of reactions. To obtain consistent results, an excess of a radical scavenger, Galvinoxyl (systematic name: 2,6-di-t-butyl-4-[(3,5-di-t-butyl-4-oxo-2,5-cyclohexa-dien-1-ylidene)-methyl] phenoxyl), was used at a molal concentration three times larger than the weight of dissolved polymer. Additionally, a gentle stream of high-purity helium was continuously bubbled into the solution to remove air and prevent its redissolution.

Degradation analysis

Molecular weight distributions of the virgin and degraded polymers were determined by g.p.c. on a Waters 150CV equipped with a triple detection scheme (differential refractomer, on-line viscometer and u.v. absorption). To cover the nearly 200-fold change in initial molecular weight, different combinations of column porosity (Ultrastyragel 10^6–10^3 Å) have to be selected. An IBM-compatible personal computer was used for data acquisition and analysis. The percentage of degraded polymer was evaluated by changes in the g.p.c. traces of the virgin and degraded samples (cf. *Figures 4* and *5*). Polymers with a molecular weight above 3×10^6 are highly prone to mechanochemical degradation. To preserve polymer integrity, extreme care should be exercised to prevent shearing during the preparation, injection and analysis of the samples. Experimental conditions for a successful g.p.c. characterization in the ultra-high molecular weight range have been described earlier[13–15]. Axial dispersion in the g.p.c. columns was calibrated with the recycling technique. True molecular weight distribution was then recovered from the g.p.c. traces by using a reshaping algorithm described by Ishige *et al.*[16].

RESULTS AND DISCUSSION

The kinetics of ultrasonic degradation is influenced by a number of parameters which are either specific to the ultrasonic wave (intensity, frequency, irradiation time), to the solvent properties (solvation quality, vapour pressure, presence of dissolved gases) or to the polymer structure (chemical composition, molecular weight). For the present investigation, we will restrict ourselves to those factors which are the most relevant for degradation kinetics modelling, i.e. the degradation time, the polymer concentration, the initial polymer molecular weight and the temporal evolution of molecular weight distributions.

Degradation as a function of sonication time

The number of broken bonds increases with the duration of sonication. Different kinetics expression have been derived in the past with the purpose of characterizing the reaction in terms of a rate constant. If degradation occurs randomly, each intact polymer chain present has the same probability of being broken in a given time interval. Chain scission should therefore follow a first-order reaction kinetics. The reality is, however, much more involved due to the large number of fracture sites and the various chain lengths present in a polymer sample. Essentially, the process of degradation could be described by a series of parallel and consecutive reactions. A polymer chain, n_i, of degree of polymerization i has $(i-1)$ bonds linking monomeric units which may be split during the reaction. The rate constant for cleavage of the jth bond is designated by $k_{i,j}$. Independently from the degradation mechanism, the fate of that polymer chain at a given time could be described by the degradation scheme shown (*Scheme 1*). The system of kinetics differential equations corresponding to *Scheme 1* is tractable only in the case of complete neglect of recombination reactions. With this simplification, the degradation kinetics equation for n_i can be written as[16]

$$\begin{aligned} dn_i/dt &= -\sum_{j=1}^{i-1} k_{i,j} n_i + \sum_{j=1}^{r-i} (k_{i+j,j} + k_{i+j,i}) n_{i+j} \\ &= -K_i n_i + \sum_{j=1}^{r-i} (k_{i+j,j} + k_{i+j,i}) n_{i+j} \end{aligned} \quad (2)$$

The maximum degree of polymerization present in the sample is r. K_i is the global scission rate constant for

$$\begin{array}{lcccl} n_{i+j} & \rightarrow & n_i & + & n_j \quad \text{(1st scission event)} \\ & & \downarrow & & \downarrow \\ & & n_l(l=1,i-1) + n_m & & \text{(2nd scission event)} \\ & & \text{etc.} & & \text{(3rd scission event)} \end{array}$$

Scheme 1

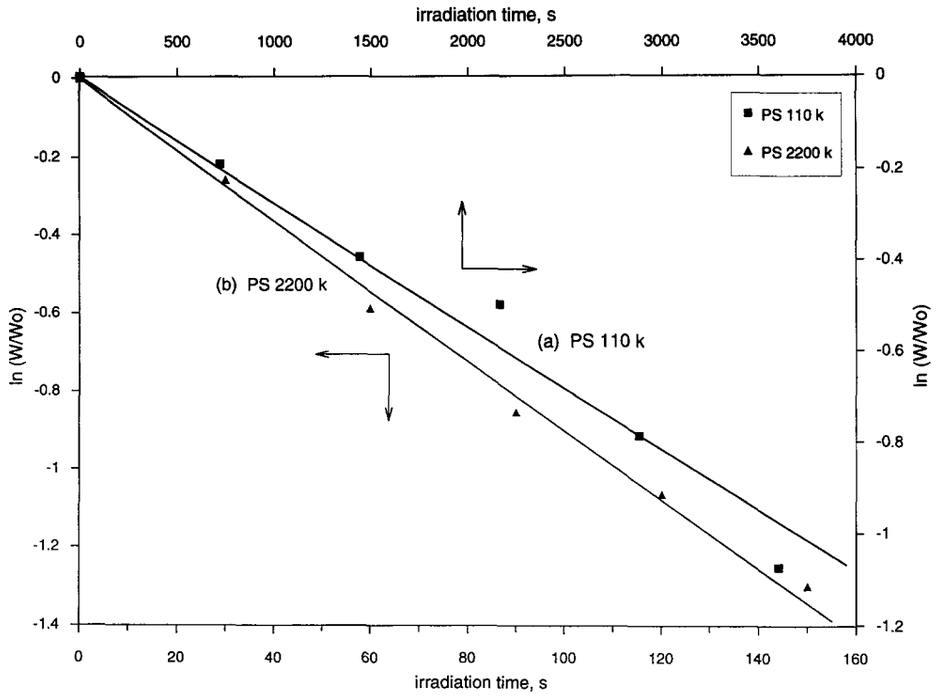

Figure 1 Semi-logarithmic plot of the dependence of degradation yield on sonication time for two selected molecular weights. Curve (a) is for $M_0 = 110 \times 10^3$ (upper abscissa); curve (b) is for $M_0 = 2.2 \times 10^6$ (lower abscissa). Solid lines are calculated according to the first-order degradation kinetics described in the text

species with degree of polymerization i, given by

$$K_i = \sum_{j=1}^{i-1} k_{i,j} n_i \qquad (3)$$

The system of first-order differential equations (2) can be exactly solved by using an analytical procedure detailed by Ballauff and Wolf[17].

If the initial polymer fraction is sufficiently narrow, it is possible to consider K as a global scission rate constant averaged over the sample molecular weight distribution (cf. *Figure 7*). Equation (2) can then be integrated to give

$$\ln(N/N_0) = \ln(W/W_0) \cong -Kt \qquad (4)$$

where N_0 and W_0 are the initial molar and molal polymer concentrations, respectively.

Results of scission kinetics calculations confirm the validity of equation (4) (*Figure 1*). To verify this relation experimentally, the fraction of undegraded polymer determined by g.p.c. is reported on a semi-logarithmic plot as a function of the irradiation time (*Figure 1*). Straight lines are obtained for the different polymer

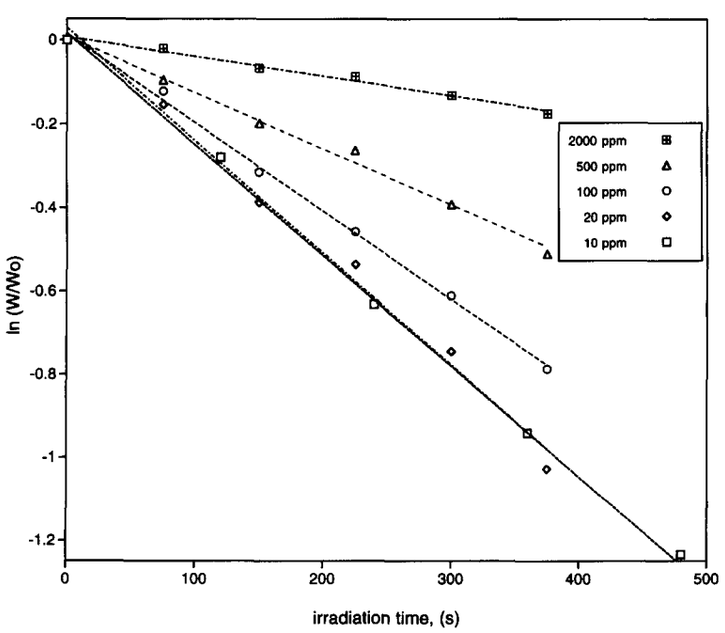

Figure 2 Effect of polymer concentration on the degradation rate for a 1.03×10^6 PS

weights up to a degradation yield of ~65%. Some deviations are observed at higher degradation extents, which can be explained partly by the increase in experimental errors in the determination of the degradation yields and partly from the approximate nature of equation (4). Apart from the molecular weight dependence, K is also a function of polymer concentration (see below). Therefore, the use of equation (4) is limited to the highly dilute regime where all molecular coils are effectively isolated from each other.

Effect of polymer concentration

The rate constant K in equation (2) should be independent from the initial polymer concentration if ultrasonic degradation is a true first-order process. Most reported results on ultrasonic degradation confirm, on the other hand, that the rate of chain breakage decreases with increasing polymer concentration[1,9]. This negative concentration dependence was attributed to a reduction in cavitation efficiency with the degree of molecular coil overlap. The effect of polymer concentration can reveal important information on the molecular mechanisms of stress transmission. Our present purpose, however, is to determine the experimental conditions where intermolecular entanglements can be avoided. With this scope in mind, we will restrict our investigations to the concentration range of 10–2000 ppm. The results, presented in *Figure 2* for two different molecular weights, reveal that the scission efficiency increases with decreasing polymer concentration but tend to level off for values below ~20 ppm. A similar trend has been observed in transient elongational flow degradation[5]. To avoid concentration effects, an initial polymer concentration of 10 ppm was used for the main experiments.

It is well known that intermolecular entanglements play a significant role in stress transmission and may, consequently, influence the rate of mechanochemical degradation. From polymer solution theory, the degree of coil overlap is controlled by the parameter $[\eta]c$, where $[\eta]$ is the intrinsic viscosity of the polymer solution. Intermolecular interactions become frequent above a critical overlap concentration (c^*) given by[18]

$$c^* \cong 1.46/[\eta] \tag{5}$$

With the Mark–Houwink coefficients for PS in decalin, it can be calculated that molecular coils start to overlap above a concentration of 12 000 and 4000 ppm, respectively, for the molecular weights of 1.03×10^6 and 8.5×10^6. From these values, it may seem surprising that polymer concentration can still influence the rate of degradation at the parts per million level. It should be recalled at this point that entanglement is a dynamic phenomenon and, therefore, depends much on the time-scale of observation. The value for c^* is derived under quiescent conditions of flow. In elongational flow, on the other hand, intermolecular interactions have been detected by birefringence as a transient polymer network at polymer concentrations two orders of magnitude below c^* [19,20].

Dependence on initial polymer molecular weight

For an initial polymer concentration below 20 ppm, the experimental slope in the linear part of the curves in *Figure 2* could be identified as the rate constant (K) for the degradation process. Most results on mechanochemical degradation reported an increase in K with the polymer molecular weight according to some empirical relation of the form

$$K \propto M^x \tag{6}$$

where the exponent x can take any value from 0 to >3, depending on the experimental conditions.

Recent theories consider mechanochemical degradation as a thermally activated stress-induced process for chain scission[21,22]. According to this model, an axial stress of the order of 5×10^{-9}–6×10^{-9} N per chain must be applied to overcome the binding potential of a carbon–carbon bond. In terms of hydrodynamic

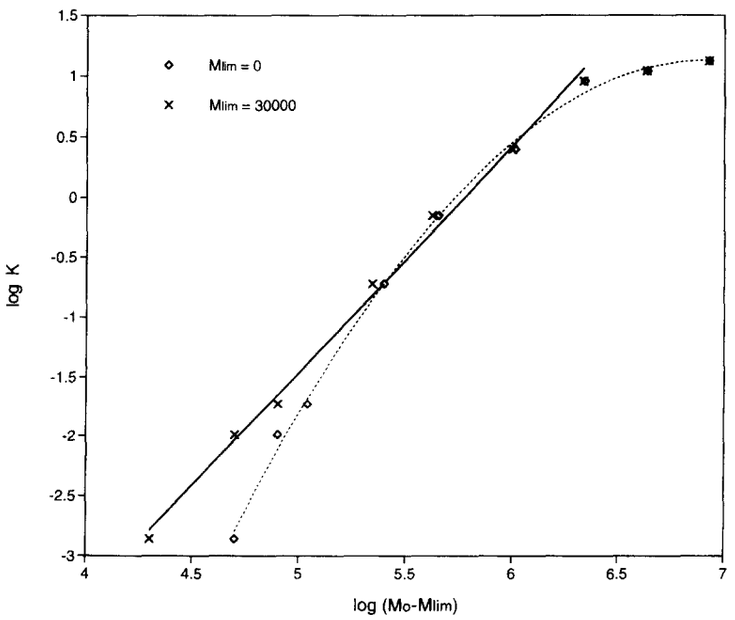

Figure 3 Double-logarithmic plot of the dependence of scission rate constant on initial polymer molecular weight (M_0, dotted line) and on ($M_0 - M_{lim}$) (full line). The empirical value for M_{lim} is 30 000

frictional loading, this minimum stress is related to a limiting molecular weight M_{lim} below which no chain scission could be observed regardless of the degradation time. When M_{lim} is included, equation (6) becomes

$$K \propto (M - M_{lim})^x \quad (7)$$

Experimentally, the double-logarithmic plot of K as a function of M fails to fit equation (6): instead of a line, a curve with a continuously changing slope from 3 to 0 was observed over the investigated molecular weight range (*Figure 3*). Better correlation was obtained with the inclusion of M_{lim}. The best fit to equation (7) was obtained with $M_{lim} = 30\,000$ Da, giving a slope $x = 1.9$ over the molecular weight range $50\,000 \leq M \leq 2.2 \times 10^6$. Above 2.2×10^6, the degradation rate becomes practically independent from M, and the slope levelled off to almost 0. This sudden change in the slope, surprising at first thought, is in fact expected on physical grounds: the degradation rate cannot increase indefinitely with M but should reach a limiting level for a given sonication power. Saturation will be observed when the probability for degradation reaches unity for any macromolecule lying in the proximity of a cavitation bubble. A more quantitative explanation will be offered in the discussion section. The limiting molecular weight is known to depend on the sonication power and other experimental factors which control the cavity collapse such as sonication frequency, dissolved gas and vapour pressure. Hence, the quoted value should be valid only under the present experimental conditions. It is, nevertheless, surprising that the same value of M_{lim} has been obtained under such diverse conditions as mechanical grinding[23], solvent freezing[24] and ultrasonication.

Probability of bond scission along the chain

Information on the bond scission probability along the chain is essential for the knowledge of the stress distribution, and hence indirectly on the molecular conformation prior to bond rupture. The localization of the bond scission position remains one of the most difficult task in polymer degradation studies. Before the advent of g.p.c., this information could only be inferred from the change of $\bar{M}_w/\bar{M}_n$ with the degradation extent[1,25]. A few studies using fractional precipitation or turbidimetric titration suggested that ultrasonic degradation was non-random with a significant propensity for midchain fracture[1]. These conclusions have since been repeatedly verified with the widespread use of g.p.c. Although g.p.c. is a highly valuable tool for the characterization of polymer degradation, it should be realized that the wealth of information concealed in the chromatograms could be usefully exploited only after extensive mathematical manipulation. Mere visual inspection of the g.p.c. traces does not provide much insight into the chain scission mechanism. For instance, the presence of a secondary low molecular weight degradation peak from an otherwise initial unimodal distribution does not necessarily mean that chain scission is non-random[25]. Even with modern high-resolution g.p.c. columns, instrumental broadening correction remains a prerequisite to recover the true molecular weight distribution, particularly with sharp polymer fractions as can be assessed from *Figure 4*. Following the nearly linear relationship between elution volume and $\log M$, the chromatogram approximately represents the semi-logarithmic plot of the differential molecular weight distribution. The non-linear molecular weight scale, however, is misleading since the distribution is distorted towards the high molecular weight fractions. For degradation modelling, only the linear plot as shown in *Figure 4* is useful for a proper evaluation of the experimental data. The molecular weight distribution clearly reveals that short fragments with $\bar{M} \leq M_0/4$ are prevalent in the degraded samples whereas chain halving is only a minor process. The presence of low molecular weight fragments even at short irradiation time suggests the existence of multiple scission action in which several covalent bonds are broken in a single degradation step.

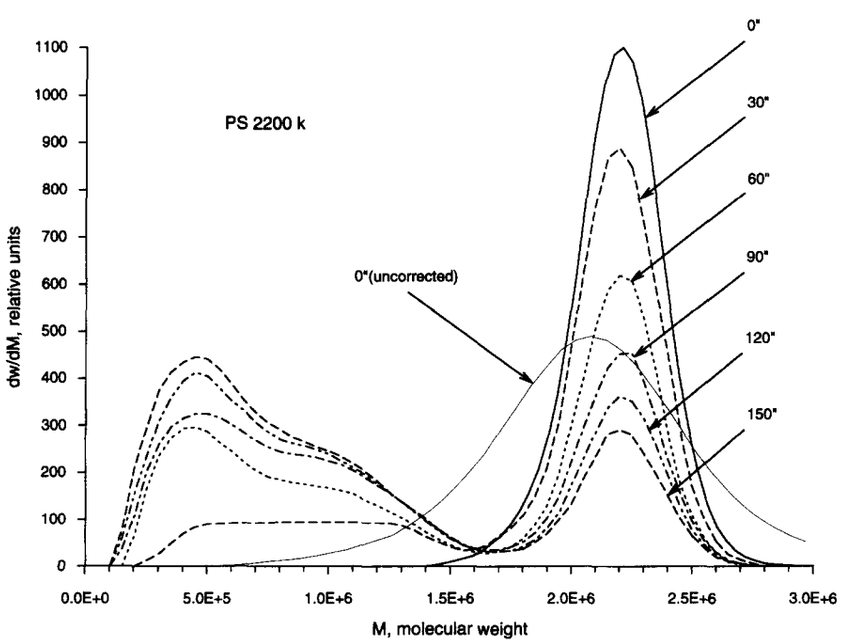

Figure 4 Change in experimental molecular weight distribution with irradiation time for a 2.2×10^6 PS. All the data are correct for axial dispersion; one example of an uncorrected curve is shown for the pristine sample

Kinetics of ultrasonic degradation

Change in the molecular weight distribution is the final outcome from a long succession of events following the application of molecular stress. Determination of the degradation mechanism from experimental molecular weight distributions is necessarily indirect and involves a trial-and-error approach. In analogy to flow-induced degradation, one can assume as a starting point that the rate of bond breakage follows a truncated central Gaussian distribution for the different positions along the chain[25]:

$$k_{i,j} = \begin{cases} C/(\sigma_i/\sqrt{2\pi})\exp[-(j-i/2)^2/2\sigma_i^2] & \text{if } i > i_{\lim} \\ \quad \text{and } j \geq i_{\lim}/2 \text{ or } j \leq i - i_{\lim}/2 & \\ 0 & \text{else} \end{cases} \quad (8)$$

with $i_{\lim}$ the number of 'quasi-monomeric' units equivalent to $M_{\lim}$.

The parameter C is adjusted to ensure that the experimental scaling law (equation (7)) is verified over the considered molecular weight range, i.e.

$$\sum_{j=1}^{i-1} k_{i,j} = C(i - i_{\lim})^{1.9} \quad (9)$$

Within a limited range of molecular weight, the relative standard deviation (R) can be considered as constant and used as a fitting parameter:

$$\sigma_i = Ri \quad (10)$$

The system of equation (2), given earlier, can be integrated after replacing the $k_{i,j}$ by the corresponding numerical values given by equation (8). Starting with the molecular weight distribution of the virgin sample, molecular weight distributions of the degraded polymer were calculated at different sonication times and compared with the experimental data. It is mandatory at this stage to consider exclusively true molecular weight distributions after appropriate axial dispersion correction. Failure to take instrumental broadening into account deteriorates the quality of the fit and may lead to an erroneous assignment of the scaling exponent (x) in equation (7).

Good agreement between the simulated and experimental data are observed only for $M_0 < 100 \times 10^3$. The quality of the fit degrades rapidly with increasing molecular weight. Deviations indicating an excess of low molecular weight fragments are already observed for $M_0 = 110 \times 10^3$ (*Figure 5*). In accord with the observations of *Figure 4*, multiple scission prevails over single scission for M in the 10^6 molecular weight range. The degradation scheme (*Scheme 1*) valid for single-scission kinetics must be modified to include the possibility for multiple scission. Techniques for computing the molecular weight distribution in the presence of multiple scission have been discussed in a recent

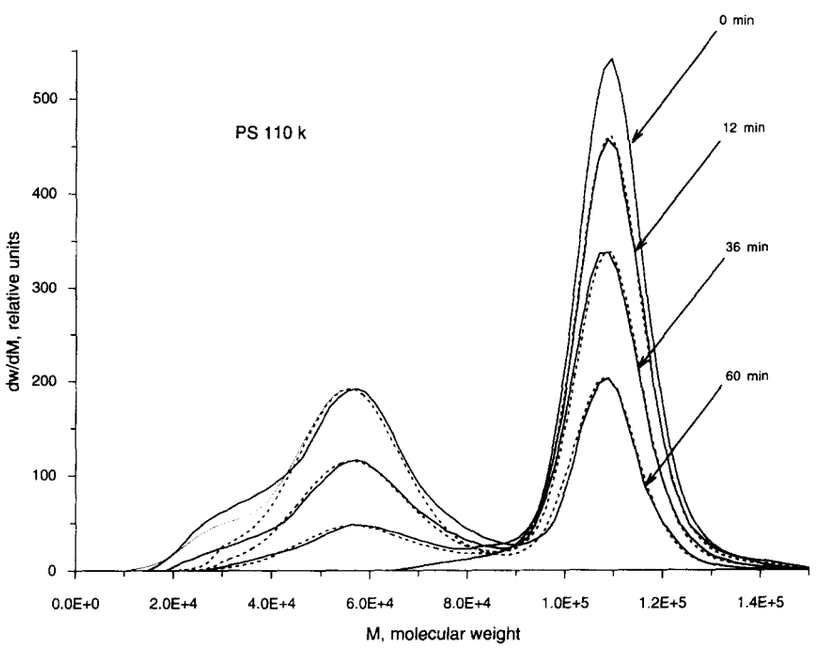

Figure 5 Experimental and simulated molecular weight distributions for a 110×10^3 PS degraded by ultrasonication at the indicated irradiation time. ——, instrumental broadening corrected, experimental data; ·····, calculated with the central Gaussian scission model with $R = 0.09$; ——, calculated with the inclusion of 10% quaternary scission

$$M_0 \xrightarrow{K_1} M_0/2 \xrightarrow{K_2} M_0/4 \xrightarrow{K_3} M_0/8, \text{ etc.} \quad \text{(Single breakup (a))}$$

$$M_0 \xrightarrow{K_1''} M_0/4 \xrightarrow{K_3} M_0/8, \text{ etc.} \quad \text{(Quaternary breakup (b))}$$

$$M_0 \xrightarrow{K_1''} M_0/8, \text{ etc.} \quad \text{(Third-order breakup (c))}$$

Scheme 2

publication[25]. For the present system, multiple scission is modelled as a succession of single-scission events. The formation of fragments with $\bar{M} \cong M_0/4$ can be formally described by the competitive reactions (a) and (b) in *Scheme 2*, whereas those with $\bar{M} \cong M_0/8$ require an additional step (c). The relative importance of each process depends on the initial polymer molecular weight. Any fragment, once formed, can be further degraded according to the same kinetics, which we have denoted as *Scheme 2*. According to the proposed degradation model, chains can only be broken in multiples of 2^n fragments (2, 4, 8, etc.). No tertiary scission, for example, as found in solvent freezing degradation, was allowed in the calculations[24]. The rationale behind the described procedure will be explained in the forthcoming section.

The influence of multiple scission on the final molecular weight distribution is shown in *Figure 6*. The best fit to the experimental data for a 2.2×10^6 PS was obtained with the following repartition: 56% of the degradation by single scission, 27% by quaternary scission ($M_0/4$) and 17% by a third-order scission process ($M_0/8$). Chain halving is practically absent for the two highest molecular weight samples, 4.34×10^6 and 8.5×10^6, whereas simultaneous scission up to the fifth-order (fragments with $\bar{M} \cong M_0/32$) have to be included for a faithful representation of the degradation results.

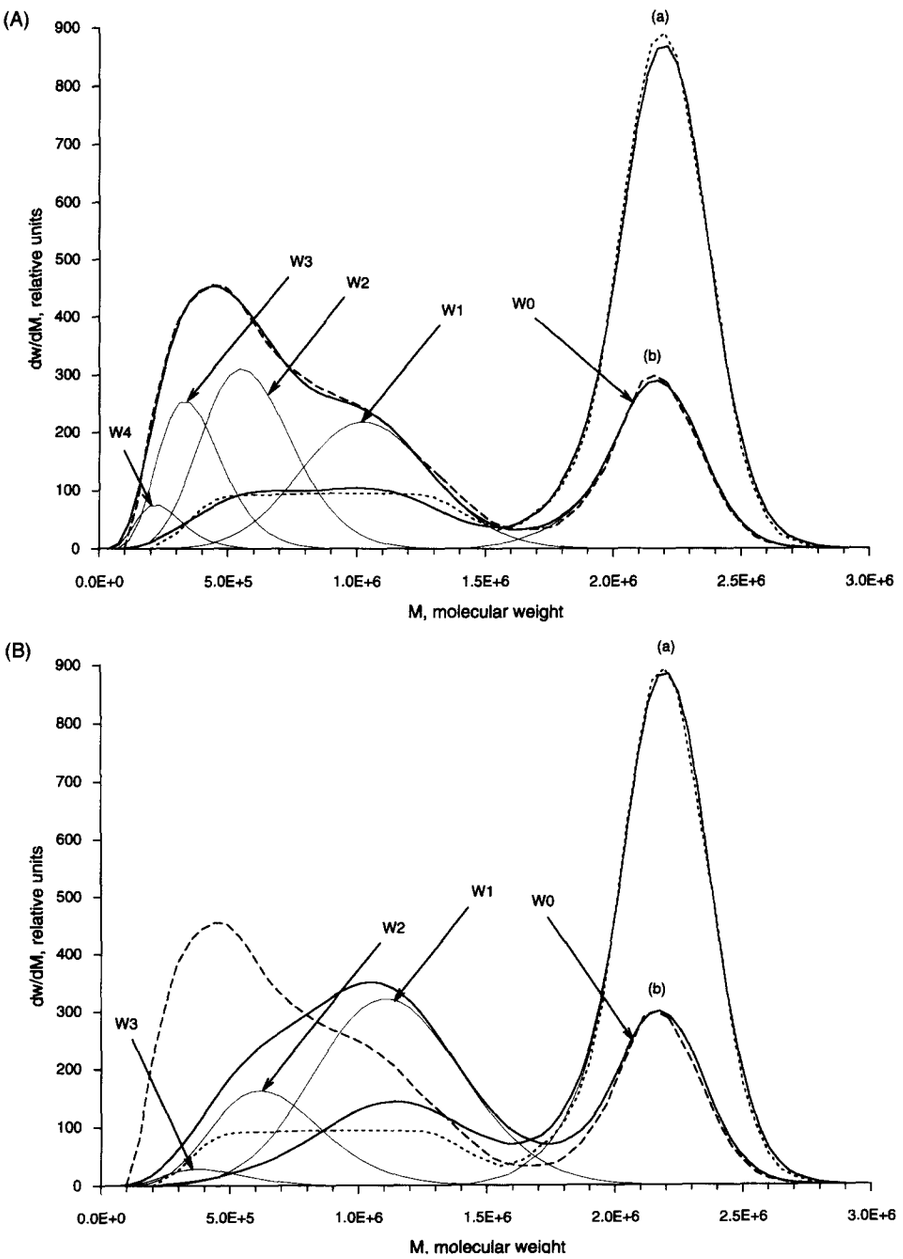

Figure 6 Simulated and experimental molecular weight distributions for a 2.2×10^6 PS degraded by ultrasonication at irradiation times of 30 s (curve a) and 150 s (curve b). The dotted lines indicate experimental data, the full lines are calculated with (A) the multiple scission model (56% single scission, 27% quaternary scission and 17% third-order scission) and (B) the central Gaussian scission model with $R = 0.13$. W_0 denotes the calculated weight fraction of all polymer chains which remain intact, while W_1, W_2, W_3, ..., refer to those fractions which have been broken once, twice, three, etc., times, respectively, at the irradiation time of 150 s

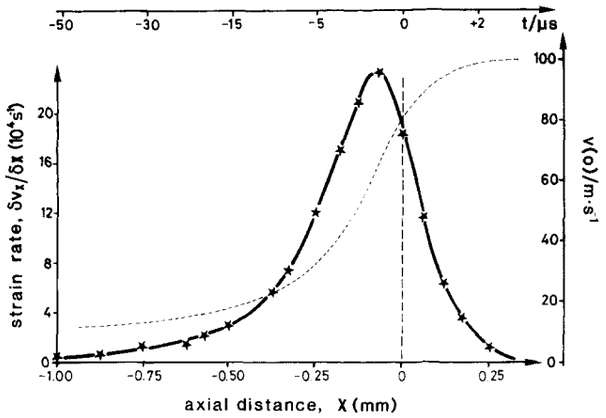

Figure 7 Elongational strain rate ($\dot{\varepsilon}_{xx} = \partial v_x/\partial x$) distribution, calculated along the symmetry axis in abrupt contraction flow. The upper abscissa indicates the transit time of a fluid element passing along the centre line. Values are given for an orifice diameter of 0.5 mm and a volumetric-average fluid velocity at the orifice of 100 m s^{-1}

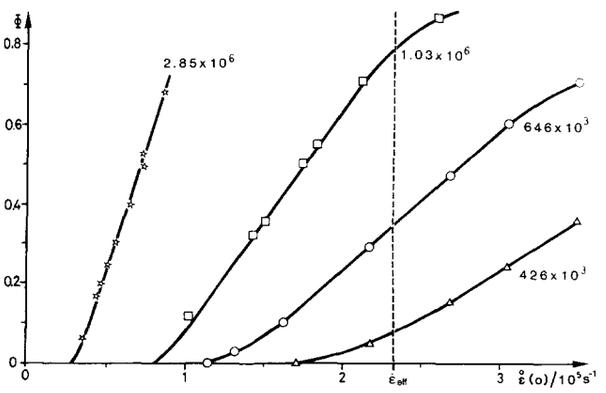

Figure 8 Dependence of the scission yield on strain rate and polymer molecular weight in transient elongational flow degradation (the numbers on the curves indicate the initial polymer molecular weight). The degradation yield for a given effective strain rate ($\dot{\varepsilon}_{eff}$) is given by the intersection of the vertical dotted line with the corresponding degradation curve

Differences between the degradation schemes (*Schemes 1* and *2*) are emphasized in *Figures 6A* and *6B*, where the weight fraction of different fragment populations are calculated and plotted for the 2.2×10^6 PS sample. Without multiple scission, short fragments are created by consecutive reactions and can only be found for extended degradation times.

ULTRASONIC AND TRANSIENT ELONGATIONAL FLOW DEGRADATION

Transient elongational flow

Transient elongational flow can be obtained by forcing a liquid across a narrow contraction[5]. As a result of the sudden change in flow cross-section, a high velocity gradient is created in front of the orifice entrance. Most of the fluid acceleration occurs in a region limited to ~1 orifice diameter and accounts for the characteristic spike-like shape of the strain rate distribution (*Figure 7*). Degradation is highly efficient in fast transient flow (*Figure 8*) and can be observed above a critical strain rate ($\dot{\varepsilon}_f$) which depends on polymer molecular weight as[26]:

$$\dot{\varepsilon}_f \propto M^{-1} \tag{11}$$

Due to the short transit time in the 'strong' flow region, molecular chains cannot accumulate sufficient strain for stretching, and it is expected that they are broken essentially in an uncoiled state. Nevertheless, precise midchain scission with relative standard deviation (R) as low as 0.07–0.08 in decalin (a poor solvent) and 0.04–0.05 in 1-methylnaphthalene (a good solvent) was observed in this type of flow (*Figure 9*)[7,12]. In comparison, chain halving with $R = 0.09$–0.13 is less precise in ultrasonication. This result, however, is not surprising in view of the extreme straining conditions prevalent during the cavity implosion.

Ultrasonic irradiation

Although the molecular mechanism for sonochemical

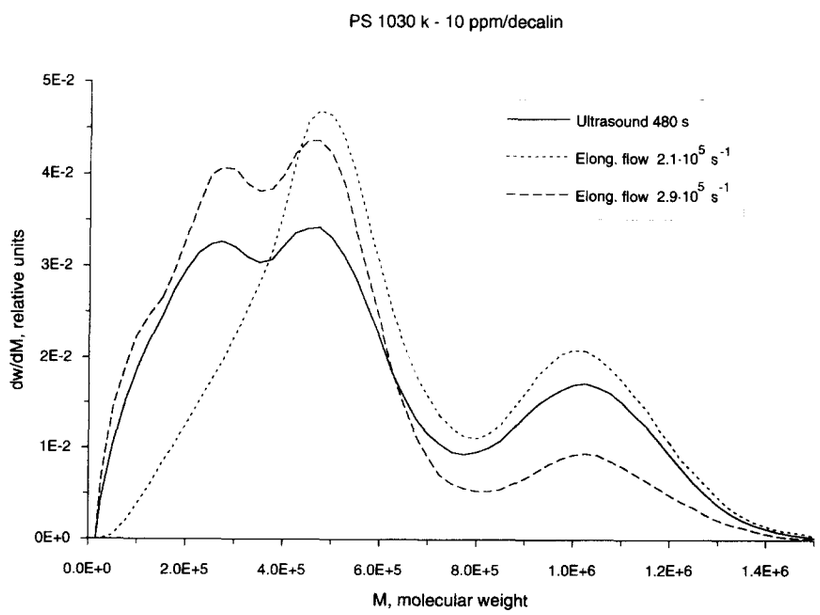

Figure 9 Comparison between the molecular weight distribution of a 1.03×10^6 PS degraded by ultrasonication for 480 s and by transient elongational flow at the indicated strain rates

degradation remains elusive, there is a general consensus that bond scission arises from the large shear gradient generated during the collapse of the cavitation bubble[9–11]. Some of the typical events which may take place during ultrasonication are recalled below (the quoted values are only order of magnitude estimates under the present experimental conditions and depend markedly on the final implosion stage).

Above a threshold sound intensity, bubbles are created and increased in size by absorption of acoustic energy until a critical diameter of the order of 250 μm is reached. The bubble becomes unstable above that size and collapses violently in a time-scale of ~20 μs (*Figure 10*). Adiabatic compression raises the internal pressure to 500 atm while the cavity temperature may attain 5800 K. A molecular coil lying next to an imploding cavity will be dragged along by the microstreams towards the bubble interior while being strained by the high fluid velocity gradient. This picture bears some resemblance to convergent flow through a constriction[5,27]. The hydrodynamics, however, is significantly different for the following reasons. First, the interior of the cavity is filled with a compressible gas with a constantly moving boundary. Secondly, the applied acoustic pressure is not constant but is a sinusoidal function of time. Following the pioneering work of Lord Rayleigh published in 1917, several mathematical treatments have been derived to describe bubble wall motion during the implosive collapse[11,28–30]. An approximate equation describing the wall velocity (v_R) is given by[11]

$$v_R = \mathrm{d}R/\mathrm{d}t = (2P_h/3\rho)^{0.5}(R_m^3/R^3 - 1)^{0.5} \qquad (12)$$

In this equation, ρ is the solvent density, P_h is the external pressure, R_m is the initial radius and R is the instantaneous radius of the imploding cavity. According to equation (12), v_R should go to infinity in the limit of $R = 0$. More detailed theoretical and experimental investigations revealed, however, that R reaches a minimum radius of the order of 0.5 μm during the final collapse[30].

Neglecting solution compressibility, the strain rate distribution can be readily computed as

$$\dot{\varepsilon}_{rr}(r) = -2v_R R^2 r^{-3} \qquad (13)$$

The strain rate distribution, calculated from equations (12) and (13) for different collapsing times, are reproduced in *Figure 10*. In contrast to transient elongational flow, the flow field during the implosion stage is time-dependent. For degradation kinetics modelling, the factor which is of importance, however, is not the spatial distribution but the temporal variation in the fluid strain rate[31]. To obtain the strain rate history of a flowing macromolecule, it is necessary to convert from the Lagrangian frame of references to an Eulerian frame which moves with the surrounding fluid element. The results of this transformation are shown in *Figures 7* and *11* for transient elongational and collapsing flow, respectively. Several experimental results, including the different scaling laws and the formation of low molecular weight fragments, can be rationalized from the curves depicted in these two figures.

First, it can be assessed from *Figure 7* that the scaling law determined in transient elongational flow has a different physical meaning from the one obtained in ultrasonic degradation. In the former case, the fluid strain rate is the controlled variable and $\dot{\varepsilon}_f$ refers to the onset value for which degradation was observed for a given polymer molecular weight. In ultrasonication, on the other hand, the limiting molecular weight and the degradation rate are dictated by an effective strain rate ($\dot{\varepsilon}_{eff}$) which prevailed during the cavity collapse. The strain rate history could not be altered excepted by changing the irradiation conditions. By extrapolating the results obtained in transient elongational flow to ultrasonic degradation, it can be deduced from M_{lim} that $\dot{\varepsilon}_{eff}$ should be $\geq 3 \times 10^6\ s^{-1}$ (*Figure 11*). Formally, the ultrasonic degradation yield for a given polymer

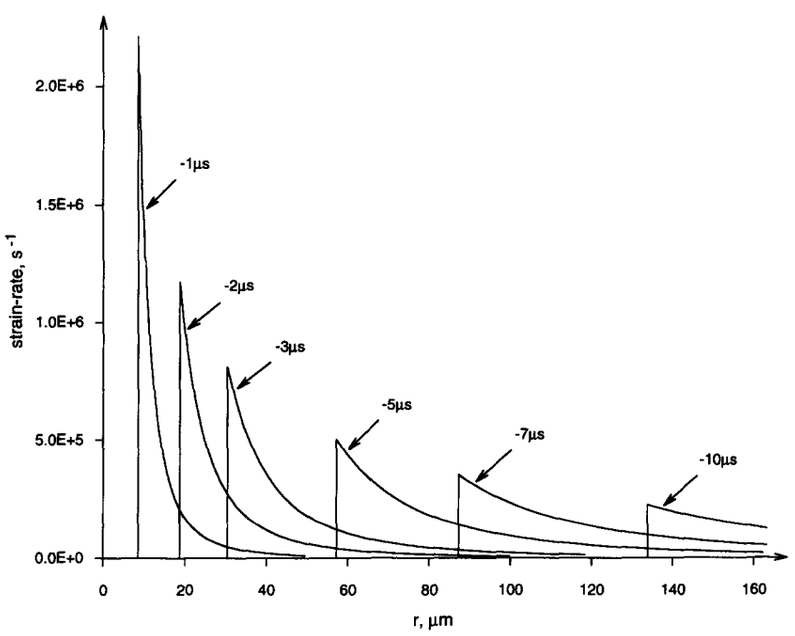

Figure 10 Strain rate distribution during a cavity collapse sketched for different implosion times. Full collapse occurs at $t = 0$; r is the distance from the cavity centre

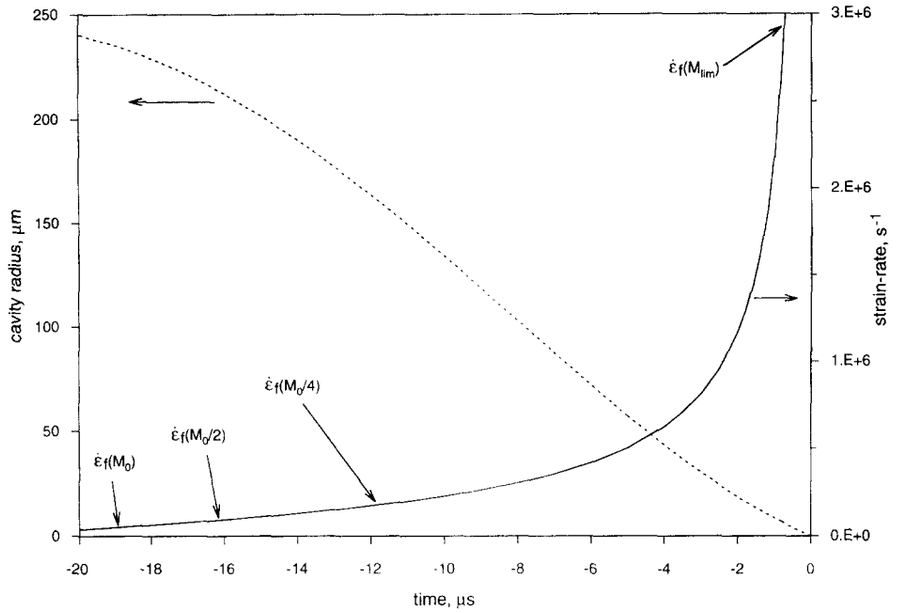

Figure 11 Temporal evolution of the bubble radius (left ordinates) Kand strain rate maximum (right ordinates) during implosion collapse

molecular weight could be obtained from the corresponding degradation curve by taking the ordinate value at the strain rate $\dot{\varepsilon}_{eff}$ (*Figure 7*). The scaling exponent x is therefore dependent on the exact value of $\dot{\varepsilon}_{eff}$ and on the shape of the degradation curves. Changes in these factors may well explain variations in the scaling exponents reported by different authors. The presently determined value of $x = -1.9$ is entirely empirical and, probably, bears no real physical meaning. In addition, since degradation tends to saturate at the same level (~90%) for all polymer samples, no change in the degradation yield with M is expected for sufficiently high polymer molecular weight: this conclusion is consistent with the experimental results reported in *Figure 3*. Multiple scission could be readily explained with the strain rate curve of *Figure 11*. During the implosion, a polymer chain lying next to a cavity is sollicitated over a wide range of strain rates with increasing magnitude. Molecular fragments formed from long polymer chains in the early implosion stage can undergo several degradation events during the cavity lifetime until either M_{lim} or total bubble collapse is reached (*Figure 11*). Similar behaviour was observed in transient elongational flow (*Figure 9*). At low strain rates, single chain halving is the predominant process. At higher $\dot{\varepsilon}$, shorter molecular chains with $\bar{M} \cong \bar{M}_0/4$ and $\bar{M}_0/8$ which stemmed from multiple scissions increased in importance, and the molecular weight distributions of the degraded polymer bear close resemblance to the one obtained by ultrasonication. In principle, the fragment population in both situations could be calculated from the strain rate history using the formalism previously developed for transient elongational flow degradation[31].

PROSPECTS AND CONCLUSIONS

In this paper, we have shown that several apparently contradicting features of ultrasonic degradation could be rationalized from the results obtained in transient elongational flow. Many of the resemblances between the two systems stem from similarities in the flow field, which is transient elongational in both situations. Due to a lack of precise knowledge of the final implosion stage, the comparison could be carried out only at a qualitative or semi-quantitative level. Recent light scattering experiments permit a single cavitation bubble to be followed throughout its history, from formation to the ultimate collapsing state[32,33]. It is anticipated that this type of experiment, when performed conjointly with degradation measurements on polymer solutions, can provide quantitative insight into the molecular mechanisms of ultrasonic degradation.

ACKNOWLEDGEMENTS

The assistance of Mr G. Yu for axial dispersion calibration is highly appreciated. The authors gratefully acknowledge financial support from the Swiss National Science Foundation.

REFERENCES

1. Casale, A. and Porter, R. S., *Polymer Stress Reactions*, Vols 1 and 2. Academic Press, New York, 1978.
2. Nguyen, T. Q. and Kausch, H. H., *Chimia*, 1986, **40**, 129.
3. De Gennes, P. G., *J. Chem. Phys.*, 1974, **60**, 5030.
4. Keller, A. and Odell, J. A., *Colloid Polym. Sci.*, 1985, **263**, 181.
5. Nguyen, T. Q. and Kausch, H. H., *Adv. Polym. Sci.*, 1992, **100**, 73.
6. Frenkel, Ya. I., *Acta Physicochim. URSS*, 1944, **19**, 51.
7. Nguyen, T. Q. and Kausch, H. H., *J. Non-Newton. Fluid Mech.*, 1988, **30**, 125.
8. Ederer, H. J., Basedow, A. M. and Ebert, K. H., in *Modelling of Chemical Reaction Systems*, ed. K. H. Ebert, P. Deuflhard and W. Jäger. Springer-Verlag, Berlin, 1981, p. 189.
9. Price, G. J., *Adv. Sonochem.*, 1990, **1**, 231.
10. Florea, M., *J. Appl. Polym. Sci.*, 1993, **50**, 2039.
11. Mason, T. J. and Lorimer, J. P., *Sonochemistry: Theory, Applications and Uses of Ultrasound in Chemistry*. Ellis Horwood, New York, 1989, Ch. 2.
12. Nguyen, T. Q. and Kausch, H. H., *Macromolecules*, 1990, **23**, 5137.
13. Nguyen, T. Q. and Kausch, H. H., Proceedings of the International GPC Symposium '91, San Francisco, CA, USA, 13–16 October, 1991, pp. 373–397.

14. Grubisic-Gallot, Z., Marais, L. and Benoit, H., *J. Polym. Sci. Part A-2*, 1976, **14**, 959.
15. Nguyen, T. Q. and Kausch, H. H., *J. Chromatogr.*, 1988, **449**, 63.
16. Ishige, T., Lee, S. I. and Hamielec, A. E., *J. Appl. Polym. Sci.*, 1971, **15**, 1607.
17. Ballauff, M. and Wolf, B. A., *Macromolecules*, 1981, **14**, 654.
18. Fujita, H., *Polymer Solutions, Studies in Polymer Science 9*, Elsevier, New York, 1990, p. 179.
19. Chow, A., Keller, A., Müller, A. J. and Odell, J. A., *Macromolecules*, 1988, **21**, 250.
20. Nguyen, T. Q., Yu, G. and Kausch, H. H., *Macromolecules*, 1995, **28**, 4851.
21. Odell, J. A., Keller, A. and Rabin, Y., *J. Chem. Phys.*, 1988, **88**, 4022.
22. Nguyen, T. Q. and Kausch, H. H., *Polymer*, 1992, **33**, 2611.
23. Mohammadi, N., Klein, A. and Sperling, L. H., *Macromolecules*, 1993, **26**, 1019.
24. Zysman, V., Nguyen, T. Q. and Kausch, H. H., *J. Polymer Sci., Polym. Phys.*, 1994, **32**, 1257.
25. Nguyen, T. Q., *Polym. Degrad. Stabil.*, 1994, **46**, 99.
26. Nguyen, T. Q. and Kausch, H. H., *J. Non-Newt. Fluid Mech.*, 1988, **30**, 125.
27. Daoudi, S. and Brochard, F., *Macromolecules*, 1979, **11**, 751.
28. Ryskin, G., *J. Fluid Mech.*, 1990, **218**, 239.
29. Kamath, V., Prosperetti, A. and Egolfopoulos, F. N., *J. Acoust. Soc. Am.*, 1993, **94**, 248.
30. Löfstedt, R., Barber, B. P. and Puttermann, S. J., *Phys. Fluids A*, 1993, **5**, 2911.
31. Nguyen, T. Q. and Kausch, H. H., *Makromol. Chem.*, 1989, **190**, 1389.
32. Gaitan, D. F., Crum, L. A., Church, C. C. and Roy, R. A., *J. Acoust. Soc. Am.*, 1992, **91**, 3166.
33. Barber, B. P. and Puttermann, S. J., *Phys. Rev. Lett.*, 1992, **69**, 3839.